Cell Oncol. (2013) 36:341–350
DOI 10.1007/s13402-013-0139-3

ORIGINAL PAPER

Visualising and quantifying angiogenesis in metastatic colorectal cancer

A comparison of methods and their predictive value for chemotherapy response

Torben Frøstrup Hansen · Boye Schnack Nielsen · Anders Jakobsen · Flemming Brandt Sørensen

Accepted: 24 June 2013 / Published online: 10 July 2013

Abstract
Purpose Angiogenesis plays an important role in tumour growth and dissemination. We have recently shown that blood vessel density, determined by image analysis based on microRNA-126 (miRNA-126) in situ hybridization (ISH) in the primary tumours of metastatic colorectal cancers (mCRC), is predictive of chemotherapy response. Here, we evaluated whether more general approaches to determine vessel density in primary tumours are equally predictive of chemotherapy response.
Methods This methodological study was carried out using paraffin embedded tissues from primary tumours of 89 patients with mCRC, who had all been treated with first-line chemotherapy (XELOX). Tissue sections from the deepest invasive tumour front were processed for miRNA-126 ISH and CD34 immunohistochemistry (IHC). Estimates of microvessel density (MVD) were obtained for both miRNA-126 and CD34 by quantitative image analyses (MVDi), vascular area per image (μm^2) analyses, and manually counting vessels in vascular hot spots (MVDh). Clinical responses were evaluated according to Response Evaluation Criteria In Solid Tumours (RECIST).
Results The MVDi for miRNA-126 showed a significant correlation with treatment response (p=0.01), with a median value of 2,071 μm^2 (95 % CI, 1,505–3,075 μm^2) in the responder group compared to 1,337 μm^2 (95 % CI, 1,038–1,499 μm^2) in the non-responder group. This difference translated into a significant difference in progression free survival (p=0.01).
Conclusions The methodological assessment of MVD and the molecular vessel marker are both important for the prediction of the chemotherapy response in mCRC. Our findings indicate that MVDi for miRNA-126 represents a powerful estimate and may serve as a clinical biomarker superior to MVDh.

Keywords Angiogenesis · Chemotherapy · Colorectal neoplasms · MicroRNA · Microvessel density · Predictive biomarkers

T. F. Hansen (✉) · A. Jakobsen
Department of Oncology, Vejle Hospital, Vejle, Denmark
e-mail: torben.hansen@rsyd.dk

A. Jakobsen
e-mail: anders.jakobsen@rsyd.dk

B. S. Nielsen
Bioneer A/S, Hørsholm, Denmark
e-mail: BSN@bioneer.dk

F. B. Sørensen
Department of Clinical Pathology, Vejle Hospital, Vejle, Denmark
e-mail: flemming.brandt.sorensen@rsyd.dk

T. F. Hansen · A. Jakobsen · F. B. Sørensen
Institute of Regional Health Research, University of Southern Denmark, Odense, Denmark

T. F. Hansen · A. Jakobsen · F. B. Sørensen
Danish Colorectal Cancer Group South, Vejle, Denmark

1 Introduction

Angiogenesis, the development of new capillaries from existing blood vessels, is a classical hallmark of cancer and affects tumour biology at different stages [1]. Several anti-angiogenetic drugs have already been approved for the treatment of malignant diseases, and additional ones are currently being tested in clinical trials. Within this context, the identification of reliable predictive biomarkers for the rational implementation of these drugs is a prerequisite. Tumour angiogenesis parameters are considered to be important for a patient's prognosis and treatment response, in the sense that the penetration of chemotherapy seems to depend primarily on the extent of the tumour vasculature [2–4]. Parameters reflecting

tumour angiogenesis may be of particular interest since the clinical benefit from anti-angiogenetic drugs should, according to the above paradigm, be related to the angiogenic activity of the tumours.

A specific visualisation of vascular endothelial cells (ECs) and a systematic and unbiased quantification of the visualised blood vessels are prerequisites for an estimate to become a reliable parameter in clinical decision making. To date, several immunohistochemical EC markers are available (i.e., factor VIII, CD31, CD34, CD105), but despite their strong associations with ECs, none of them seems to be EC-specific [5–11]. Antibody cross-binding or unspecific antibody interactions in general represent additional obstacles in the immunohistochemical visualisation of ECs [12, 13]. An interesting alternative to the immunohistochemical detection of ECs is the identification of EC-specific microRNAs (miRNAs). MicroRNAs are small non-coding RNAs with the ability to modulate gene expression at the post transcriptional level [14, 15]. The field of miRNA research has gained considerable interest in recent years, due to its increasingly recognized role in modulating tumour behaviour, including the de-novo formation of tumour blood vessels [16, 17]. MicroRNAs can be detected in tissue sections by in situ hybridization (ISH) using high affinity Locked Nucleic Acid-DNA (LNA-DNA) chimeric probes [18]. MicroRNA-126 has in the recent past been identified as an EC-specific miRNA, affecting vascular endothelial growth factor A (VEGF-A)-mediated cell signalling, suggesting a pivotal role of this miRNA in the angiogenetic process [19–21]. Currently, the vast majority of the literature on miRNAs and their role in cancer development is based on in vitro studies and experimental animal studies. Since the functions of miRNAs are likely to be tumour and/or tissue-specific, tissue-based studies of patients with cancer are necessary for this knowledge to be implemented into future clinical treatment strategies. Assessing angiogenesis in tumour sections may also provide additional information on tumour biology and may open up the way to perform large scale biomarker validation studies. The above mentioned problems related to the specific detection of ECs using immunohistochemistry (IHC) are, however, also relevant to miRNA ISH [18, 22] and, as such, call for further elucidation. In a previous study, using the EC-specific miRNA-126 in a quantitative ISH assay, we found that this visualisation technique provided novel, clinically meaningful information [23] that, if validated, could prove valuable in the development of a predictive bio-marker.

The quantification of stained vascular structures in tissues is, in turn, also associated with technical obstacles. In the past, the microvessel density (MVD) method has been established as the preferred technique. Microvessels are usually assessed in the most vascularised areas of the tumour sections (so-called hot spots), based on the assumption that they provide the optimal estimate of the angiogenic activity. The MVD technique is, however, observer dependent and may be subject to considerable intra- and inter-observer variability [24]. Computer guided image analysis, on the other hand, represents a less observer dependent approach allowing a more systematic quantification and, thus, enabling the attainment of unbiased and more reproducible results [24]. The current evidence seems to support the use of MVD as a prognostic marker in patients with colorectal cancer (CRC) [6, 25, 26], but its putative role as a predictive biomarker for treatment response is less well studied.

We have previously shown that estimates of MVD, determined by miRNA-126 ISH and quantified by image analysis in the primary tumours from patients with metastatic CRC (mCRC), was predictive for response to first-line chemotherapy [23]. Here, we evaluated whether more general approaches to determine MVD in the primary tumours may provide an equally predictive value. Estimates were obtained from the deepest invasive tumour front for both miRNA-126 and CD34 by quantitative image analysis (MVDi), and by manually counting vessels in vascular hot spots according to the established MVD technique (MVDh, Fig. 1).

2 Material and methods

2.1 Study population

The present study includes a consecutive cohort encompassing 89 patients with mCRC histologically verified at the Department of Clinical Pathology, Vejle Hospital, Denmark. First-line chemotherapy (XELOX, see below) was initiated in the period from May 2004 to December 2009. None of the patients with rectal cancer had received preoperative chemoradiation. Survival data from patients with previous cancer diagnoses, but no sign of relapse at the time of their CRC diagnosis (n=2), were left uncensored. Progression free survival (PFS) data from ten

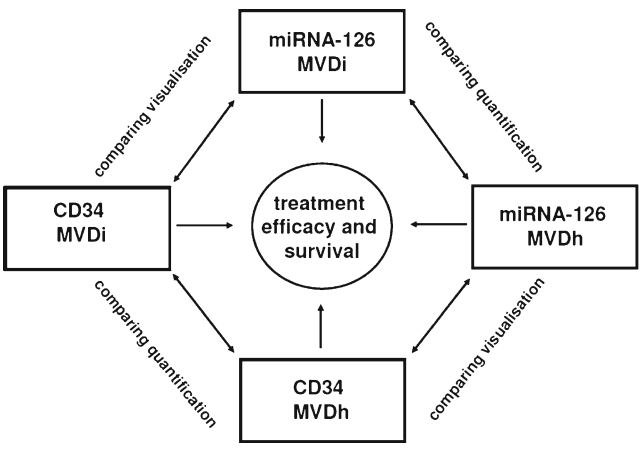

Fig. 1 Diagram illustrating the design and aim of the study. *MVDi* microvessel density estimated by quantitative image analyses, *MVDh* microvessel density estimated by manually counting vessels in vascular hot spots

patients were censored based on initiation of second-line treatment or local interventions, such as radiofrequency ablation or surgical resection of liver metastases (data were censored from the day of the intervention). The study was approved by the Regional Scientific Ethical Committee for Southern Denmark according to Danish law, J.nr. S-VF-20040047, and informed consent was obtained from all patients enrolled in the study.

2.2 Treatment regimen

All patients received XELOX, including a 2-hour intravenous infusion of oxaliplatin 130 mg/m^2 on day 1 followed by oral capecitabine 1,000 mg/m^2 twice daily on days 1 through 14 (28 doses) in a 21-day cycle. The treatment was discontinued in case of disease progression. None of the patients experienced unacceptable toxicity.

2.3 Evaluation and tumour response criteria

Treatment responses were evaluated according to the Response Evaluation Criteria In Solid Tumors (RECIST) (version 1.0) every 9 weeks. Responding patients were classified as having either a complete response (CR) or a partial response (PR). Patients with stable disease (SD) or progressive disease (PD) were defined as non-responders. All CT scans were evaluated during the course of the treatment and re-evaluated by one of the investigators (TFH) in relation to the current study.

2.4 Histological specimens

Immediately after surgery the removed bowel segment, containing the primary tumour, was transferred to the Department of Clinical Pathology where a pathologist performed standard sampling. All samples followed routine formaldehyde fixation and paraffin embedding (FFPE). The tumours were histologically classified (WHO) and staged according to the pTNM system. Paraffin blocks containing the tumour periphery with the deepest invasive site were selected for this study. The tissue sections for IHC and ISH were obtained from the same paraffin block in the closest possible proximity of each other.

2.5 MicroRNA-126 in situ hybridization

MicroRNA-126 ISH was performed as previously described [18, 22]. In brief, ISH was carried out using a one-day protocol on a Tecan Freedom Evo automated hybridization instrument (Tecan, Männedorf, Switzerland) [22]. All FFPE tissue sections were 6-μm thick and processed on two separate days. A double digoxigenin (DIG)-labelled miRCURY Locked Nucleic Acid (LNA) probe (LNA^{TM} microRNA detection probe, Exiqon, Denmark) specific for human miRNA-126 was used. The DIG-labelled probe was detected with alkaline phosphatase conjugated sheep anti-DIG Fab fragments followed by 4-nitro-blue tetrazolium (NBT) and 5-brom-4-chloro-3′-Indolyl-phosphate (BCIP) chromogenic staining and nuclear fast red counterstaining.

2.6 CD34 immunohistochemistry

The CD34 immunostaining was performed as previously described [27]. In brief, 4-μm thick FFPE sections were deparaffinised using heat-induced epitope retrieval in Tris EGTA (TEG) buffer at ph 9. Next, endogenous peroxidase was blocked with hydrogen peroxide and the sections were incubated with anti-CD34 mouse monoclonal antibody (CD34 Class II, clone QBEnd 10, M7165, Dako, Denmark) diluted 1:400 and, subsequently, visualised using the Super Sensitive IHC Detection System (BioGenix, Fremont, CA, USA). This procedure was followed by incubation in a solution of Tris-buffered Saline (TBS) containing 0.5 % copper sulphate to intensify the DAB chromogene. Finally, the sections were counterstained with haematoxylin. The CD34 immunostainings were performed manually. The same anti-CD34 monoclonal antibody was used for the entire cohort, but the Biogenex detection system involved two different lots (approximately half of the patients with each lot).

2.7 Microvessel density counting by the hot-spot method (MVDh)

Tumour sections stained for miRNA-126 and CD34 were assessed for the presence of hot spots at 40× and 100×, and counting of microvessels was performed at 200× through microscope oculars using an inserted counting grid. Any stained EC or EC cluster clearly separated from adjacent microvessels by tumour cells and/or stromal elements was considered a single, countable microvessel. Vessel lumen was not required for a structure to be counted as a microvessel. Counting was performed in three hot spots in each section, using an unbiased counting frame with an area of 0.07 mm^2, and the mean MVD (MVDh) was used for data analysis. Microvessels were counted at the deepest invasive tumour front by one observer (TFH) unaware of the patient outcome. The inter-observer reproducibility related to this technique has previously been reported, with r=0.80 and p<0.0001 [27].

2.8 Microvessel density counting by image analysis (MVDi)

MicroRNA-126: The Visiopharm integrated microscope and software module (Visiopharm, Hørsholm, Denmark) were used for image analysis. Initially, the deepest invasive tumour front, corresponding to the 1.5 mm tumour periphery, was marked (Fig. 2). Ulcerating, necrotic, and normal tissue areas were avoided. For image analysis, up to 20 random, systematically

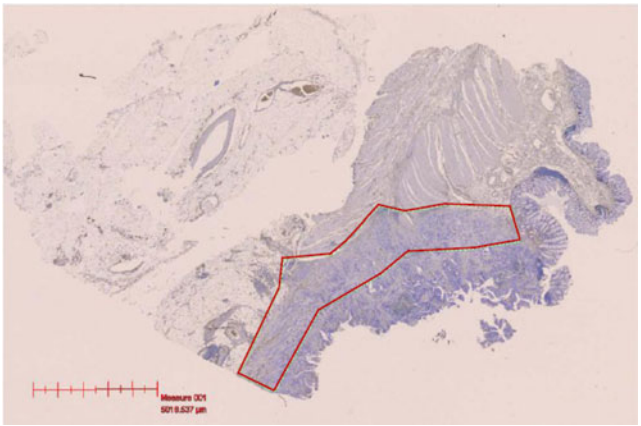

Fig. 2 Sampling of cancer area for determination of MVD by image analysis (MVDi). Representative tissue section with normal colonic epithelium, invasive cancer and adjacent submucosa and muscular coat. A tissue area of the tumour periphery (depth 1.5 mm) containing the deepest invasive tumour front was marked in which systematic random selection of up to 20 images was obtained for the data analyses. The section presented was stained for CD34 (see Fig. 3) and counterstained with hematoxylin

positioned images (282× total magnification on the computer monitor) were collected from the marked area corresponding to at minimum 5 % of the entire invasive front. Only images with cancer cells and tumour stroma were included and images containing distorted tissue and staining artefacts were excluded. Tumour structures with gland-like lumen, some of which contain necrotic debris, were present in the images for the MVDi analyses, but constituted a minor fraction of the total area. Tumour cells were clearly identified when they constituted 5–10 % of the image. In general the images contained 30–70 % cancer cells and 30–70 % stroma. A corresponding pixel classifier was designed and included the following colours for identification of the stained histological structures: strong blue (the ISH signal), weak blue (background ISH signal), red (nuclear stain), and unstained (no-tissue and erythrocytes). The strong blue area of the ISH signal (i.e., vascular area in μm^2 per image) was used as the parameter reflecting miRNA-126 MVD, and the mean score from the sampled images was calculated for each patient (MVDi). The same pixel classifier was used for all 282× images using batch processing. Five cases were excluded due to a limited number of images (less than 10 images). Figure 3a shows the underlying pixel classifier for miRNA-126. The image analysis protocol was performed by one observer (BSN) unaware of the clinical results.

CD34: For image analyses of CD34 the same principles were followed as for miRNA-126. The image acquisition configuration was the same, but another pixel classifier discriminating DAB chromogen from haematoxylin was developed. Parameters for the CD34 stained sections included intense DAB (strongly stained specific DAB reaction), weak DAB (medium stained specific DAB reaction), blue counter stain (haematoxylin), and unstained area (no tissue and erythrocytes). As for the miR-126 assessment, the same pixel classifier was used for all 282× images through batch processing. The area of the strong + medium DAB signals (μm^2 per image) was used as the parameter reflecting CD34 MVDi, and the mean score from the sampled images (at 20× magnification) was used for each patient. Figure 3b shows an example of the underlying pixel classifier. We noted a difference in the staining intensities for the two antibody detection lots. Therefore, a ratio consisting of the average mean score for each patient sample detected with lot number one and number two was calculated. This ratio was used for normalisation of the scores from lot number one in order to obtain comparable scores for the entire cohort. Performing all the statistics with non-normalised data from the two lots individually did, however, not change any of the presented results.

2.9 Statistical analysis

Median values were compared using the Wilcoxon rank sum test. The progression free survival (PFS) was defined as the time from start of treatment until the first documented tumour progression or death by any cause. The overall survival (OS) was defined as the time from start of XELOX therapy until death by any cause. All patients were successfully followed and the survival data were complete. The log rank test was used to test for differences between the groups. All statistical calculations were carried out using the NCSS statistical software package (NCSS Statistical Software, Kaysville, UT 84037, USA, version 2007). P values <0.05 were considered significant, and all tests were two-sided.

3 Results

3.1 Visualisation of EC structures

Endothelial cell (EC)-derived structures were successfully visualised in the vast majority of all tissue sections. The miRNA-126 probe resulted in a strong ISH signal in vessels, while only sparse, unspecific staining was detected in the surrounding tissues (Fig. 3a). Background signals were detected in a few samples. Correspondingly, CD34 immunohistochemical visualisation resulted in strong signals from tumour vessels, while unspecific staining of non-ECs was detected in a few cases (Fig. 3b).

3.2 Correlation between MVD and patient characteristics

Patient characteristics along with the four microvessel density (MVD) estimates are listed in Table 1. These data revealed a significant correlation between the number of metastatic organ sites and the median miRNA-126 MVDi. Thus,

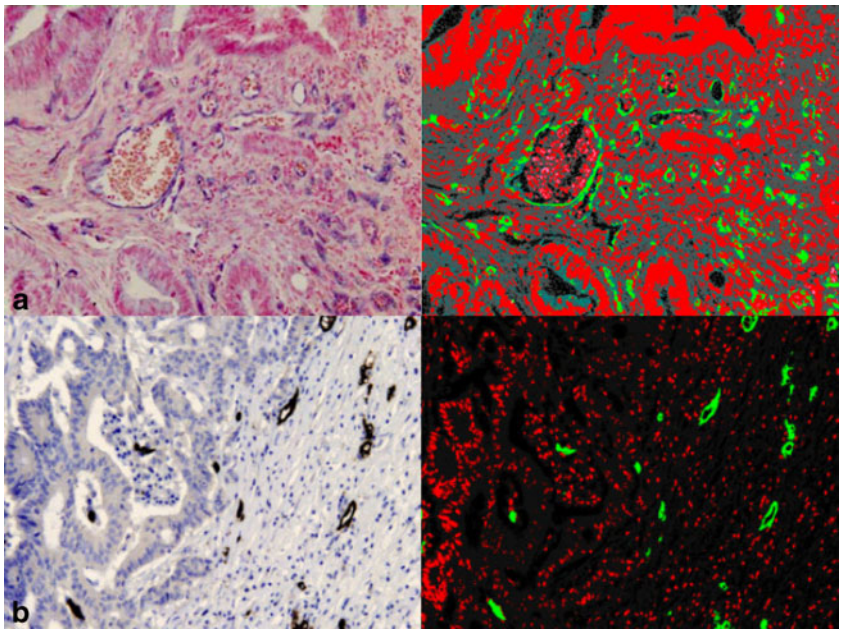

Fig. 3 **a** MicroRNA-126 positive structures (*left*) visualised by in situ hybridization in a tissue section from a patient with colon cancer and the corresponding pixel classifier (*right*) used for image analyses. The image is one of many sampled images collected from each tumour. **b** Immunohistochemical visualisation of CD34 positive structures (*left*) in another tissue section from the same patient and the corresponding pixel classifier (*right*)

the presence of two or more metastatic organ sites was related to a lower density in the primary tumour of miRNA-126 MVDi compared to the miRNA-126 MVDi in patients with metastases limited to one organ site ($p<0.001$). Furthermore, our data revealed that patients with high CD34 MVDh values significantly more often carried microsatellite stable (MSS) tumours ($p=0.01$).

3.3 Relationships between the four angiogenic estimates

The relationships between the four MVD estimates were analysed with both the visualisation method and the quantification method held constant. This approach resulted in four correlation analyses as illustrated in Fig. 4. In general, the correlations were weak and only in two situations they resulted in significant ($p<0.05$) or nearby significant ($p=0.05$) results, i.e., when image analyses were held constant (miRNA-126 MVDi versus CD34 MVDi) and when CD34 visualisation analyses were held constant (CD34 MVDh versus CD34 MVDi).

3.4 Relationship with treatment response and survival

Five patients were excluded, as they had received XELOX as second or third line treatment. One patient was excluded because of insufficient response evaluation according to the RECIST criteria (this patient was also excluded for the following reason). Four additional patients were excluded from the miRNA-126 MVDi analysis because the invasive tumour fronts in their tissue sections were of inadequate size for image analysis in order to provide a reliable estimate (Table 2). The median miRNA-126 MVDi was significantly higher in the responding patients, 2,071 μm^2 (95 % CI, 1,505–3,075 μm^2) compared to the non-responding patients, 1,337 μm^2 (95 % CI, 1,038–1,499 μm^2), $p=0.01$. None of the remaining three MVD estimates were related to treatment response. To assess the predictive value of miRNA-126 MVDi, patients were divided into two groups. The median value (2,071 μm^2) from the response group was used as cut-off. By applying this strategy, the predictive value of a positive test (>2,071 μm^2) was 18/26=69 %, and of a negative test (<2,071 μm^2) 36/53=68 %.

In order to assess the possible prognostic value of the MVD estimates, a two group comparison was applied using median values from the respective estimates as cut-off (Table 3). The median overall survival for the entire cohort ($n=89$) was 18.5 months (95 % CI, 16.7–21.8 months). The results of miRNA-126 MVDi and treatment response yielded a significant difference in PFS, $p=0.01$. The median PFS for patients with a high miRNA-126 MVDi was 8.9 months (95 % CI, 7.4–9.8 months) compared to 6.2 months (95 % CI, 4.3–6.9 months) for patients with a low miRNA-126 MVDi. The difference in PFS also translated into a tendency difference in OS, $p=0.06$. Similarly, as observed for the treatment response, none of the other three MVD estimates investigated were related to survival. Subgroup analyses based on tumour localization and stage at the time of diagnoses did not alter any of the presented results.

4 Discussion

Angiogenesis is important for the growth of a malignant tumour and for several steps to be taken in the metastatic process. These aspects have become increasingly important in

Table 1 Patient characteristics related to miRNA-126 and CD34 derived estimates

	Number (%)	miRNA-126 MVDi (μm^2) (n=84)[a]		CD34 MVDi (μm^2) (n=89)		miRNA-126 MVDh (counts) (n=89)		CD34 MVDh (counts) (n=89)	
	(n=89)	Median (95 % CI)	p-value	Median (95 % CI)	p-value	Median (95 % CI)	p-value	Median (95 % CI)	p-value
Sex									
Male	45 (51)	1462 (1009–2071)	0.65	4170 (3435–4979)	0.22	9.3 (8.3–10.3)	0.78	13.0 (12.0–14.0)	0.10
Female	44 (49)	1603 (1291–1980)		3423 (3170–4286)		9.2 (8.3–10.0)		12.2 (10.7–13.0)	
Age (years)									
Mean (SD)	63.2 (8.2)								
Range	24–80								
>mean	49 (55)	1578 (1244–2009)	0.88	3820 (3306–4649)	0.34	9.0 (8.3–9.7)	0.13	13.0 (12.3–14.0)	0.08
<mean	40 (45)	1469 (1038–2272)		3480 (3170–4645)		9.7 (8.7–10.7)		11.4 (10.7–13.0)	
ECOG PS									
0	37 (42)	1534 (1146–1980)	0.56	3518 (3180–4741)	0.84	9.7 (8.7–11.0)	0.43	12.3 (10.7–14.0)	0.62
1–2	52 (58)	1475 (1063–2009)		3720 (3193–4312)		9.0 (8.3–9.7)		12.9 (11.7–13.7)	
Localization									
Rectum	18 (20)	1624 (747–3778)	0.87	4145 (3180–5103)	0.46	9.0 (6.7–10.0)	0.38	13.9 (11.0–16.3)	0.14
Colon	71 (80)	1502 (1328–1973)		3637 (3182–4312)		9.3 (8.7–10.0)		12.7 (11.7–13.0)	
Left colon	47 (66)	1419 (1009–1973)	0.41	3306 (3133–3943)	0.12	9.3 (8.7–10.3)	0.95	13.0 (11.7–13.7)	0.39
Right colon	24 (34)	1675 (1291–2273)		4448 (3175–5230)		9.5 (7.3–10.3)		11.7 (10.7–13.0)	
MSI status[b]									
MSI	8 (11)	2261 (304–5690)	0.32	4053 (2691–6031)	0.75	8.0 (6.0–11.0)	0.45	10.8 (8.0–12.7)	**0.01**
MSS	62 (89)	1519 (1328–1863)		3676 (3195–4570)		9.7 (8.7–10.0)		13.5 (12.3–14.0)	
Metastatic sites[c]									
1	27 (31)	2129 (1654–3366)	**<0.001**	3727 (3144–5009)	0.86	9.7 (6.7–11.0)	0.61	12.7 (10.7–14.0)	0.77
≥2	59 (69)	1337 (812–1532)		3637 (3195–4570)		9.0 (8.3–9.7)		12.7 (11.7–13.7)	

P-values in bold are below the limit of significance (p<0.05)

CI confidence interval, *MVDi* microvessel density estimated by quantitative image analyses, *MVDh* microvessel density estimated by manually counting vessels in vascular hot spots., *SD* standard deviation, *ECOG PS* Eastern Cooperative Oncology Group performance status, *MSI* microsatellite instable, *MSS* microsatellite stable

[a] Five cases were excluded due to a limited number of images (less than 10 images)

[b] MSI status was not assessed in all patients

[c] A reliable estimate of the number of metastatic sites was not possible in 3 patients according to the RECIST criteria

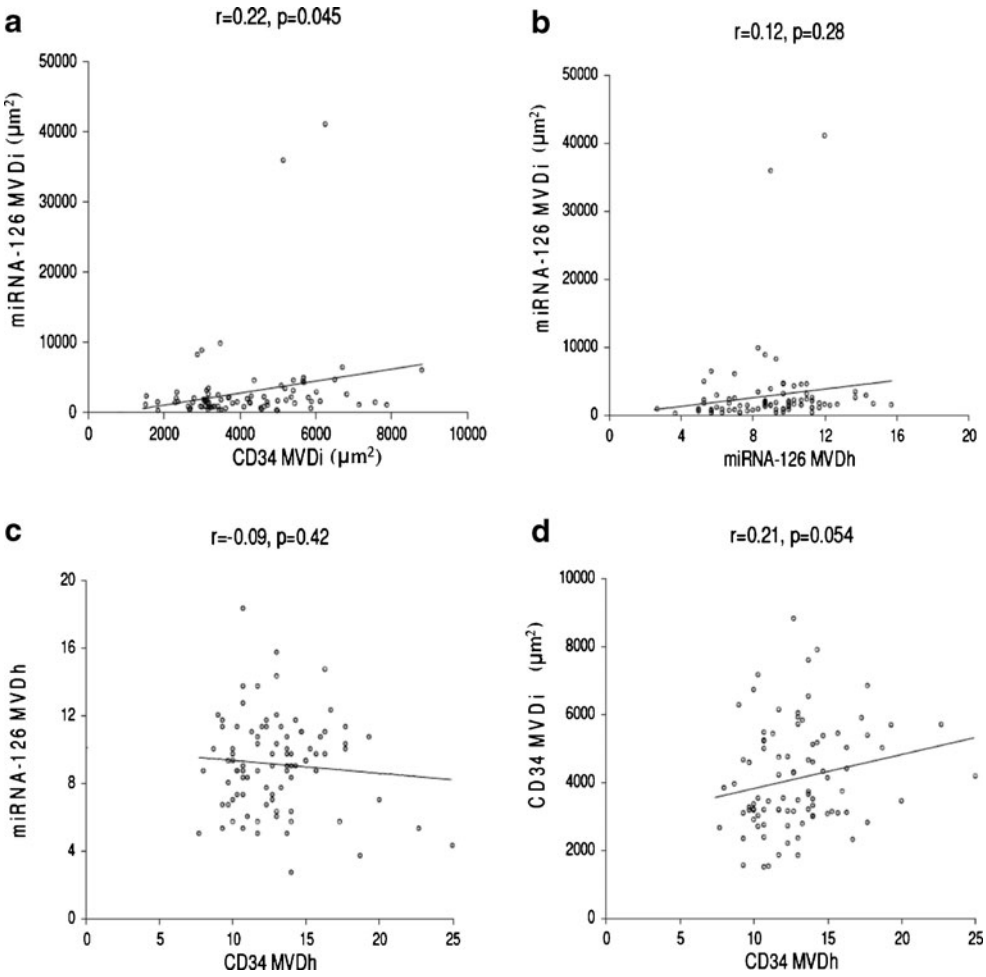

Fig. 4 **a–d** Linear regression comparing the four estimates based on visualisation (miRNA-126 or CD34) and quantification (image analyses or conventional microvessel counting (MVD)) (n=84 in **a** and **b**, n=89 in **c** and **d**)

daily clinical practise, especially after the introduction of anti-angiogenetic drugs. Our knowledge on this tumour feature is constantly growing, but we still fail to understand why anti-angiogenetic drugs are beneficial for instance in a metastatic setting [28], but not in an adjuvant setting [29]. Reliably estimating the clinical relevance of angiogenesis is essential for dealing with this challenge. Here, we showed that among the four different microvessel density (MVD) estimates tested, the miRNA-126 positively stained microvessel estimate, quantified by image analysis (miRNA-126 MVDi), was the only one to predict response to first-line XELOX treatment in a cohort of patients with metastatic colorectal cancer (mCRC). It is surprising that the traditional MVD estimates, based on the same visualisation technique but quantified differently, did not result in more convincing correlations. Different sizes of the areas used for quantification and differences in the

Table 2 Angiogenic estimates in relation to response to treatment

Estimate	Response		
	Yes (n=37) Median (95 % CI)	No (n=46) Median (95 % CI)	p-value
miRNA-126 MVDi	2071 (1505–3075)	1337 (1038–1499)	**0.01**
miRNA-126 MVDh	9.7 (8.7–10.3)	9.0 (7.7–10.0)	0.34
CD34 MVDi	3714 (3180–5154)	3672 (3129–4583)	0.57
CD34 MVDh	12.7 (10.7–14.0)	13.0 (11.7–13.7)	0.70

P-values in bold are below the limit of significance (p<0.05)

Yes positive response to treatment, *No* no response to treatment, *CI* confidence interval, *MVDi* microvessel density estimated by quantitative image analyses, *MVDh* microvessel density estimated by manually counting vessels in vascular hot spots. (n=79 in the miRNA-126 MVDi comparison, n=83 in the remaining three comparisons (for excised cases see text))

Table 3 Angiogenic estimates in relation to survival

	Progression free survival (PFS)			Overall survival (OS)		
Estimate (median)	Events/median PFS (months)	HR (95 % CI)	*p*-value	Events/median OS (months)	HR (95 % CI)	*p*-value
miRNA-126 MVDi						
<1519	36/6.2	1		40/16.8	1	
>1519	29/8.9	0.54 (0.33–0.88)	**0.01**	33/21.8	0.65 (0.41–1.03)	0.06
miRNA-126 MVDh						
<9.3	35/7.1	1		44/18.9	1	
>9.3	33/7.1	0.99 (0.62–1.60)	0.98	32/17.3	0.93 (0.59–1.46)	0.76
CD34 MVDi						
<3714	38/7.1	1		41/19.1	1	
>3714	30/7.2	0.84 (0.52–1.35)	0.47	35/16.9	1.04 (0.66–1.63)	0.88
CD34 MVDh						
<12.7	36/6.8	1		42/18.2	1	
>12.7	32/7.4	0.78 (0.48–1.26)	0.30	34/18.5	1.21 (0.77–1.92)	0.39

P-values in bold are below the limit of significance ($p<0.05$)

HR hazard ratio, *CI* confidence interval, *MVDi* microvessel density estimated by quantitative image analyses, *MVDh* microvessel density estimated by manually counting vessels in vascular hot spots

Total number of events is smaller for the miRNA-126 MVDi analyses due to the removal of data from four patients caused by insufficient image sampling. (PFS and OS comparisons: $n=79$ and $n=84$ with regard to miRNA-126 MVDi, $n=83$ and $n=89$ with regard to the remaining three estimates (for details, see text))

magnification between the two techniques may explain some of this divergence. The only estimates with a significant overall correlation were miRNA-126 MVDi and CD34 MVDi. This may indicate a superior reproducibility of the image guided quantification technique compared to the MVD technique based on the subjective quantification in hot spots (MVDh). Our results also clearly revealed the difficulties in obtaining reliable MVD estimates and how different methodological approaches may profoundly affect the final conclusions. In this study the miRNA-126 MVDi and CD34 MVDi estimates were obtained exclusively from images of the invasive tumour front. This was done to allow a direct comparison with the MVDh estimates, which were also obtained from the invasive front zone.

We found that the group of responding patients generally exhibited higher miRNA-126 MVDi estimates, which is in agreement with our previous findings based on MVDi estimates obtained from the entire tumour area [23]. Together, these observations suggest that the miRNA-126 related microvessel integrity is not limited to specific tumour compartments. The two estimates based on CD34 visualisation showed no relationship with treatment response. This may be related to CD34 being a less specific EC marker as compared to miRNA-126. It does not explain, however, why the miRNA-126 MVDh estimate was not related to response. One reason may be that, although a specific visualisation of EC-derived structures was achieved, the use of a more observer-dependent quantification method, such as MVDh, may render the final estimate invalid with respect to treatment efficacy. Furthermore, the smaller area fraction of the invasive front used for quantification with the MVDh technique may render this estimate less representative for the entire invasive front.

We noted an interesting association between low miRNA-126 MVDi estimates and increased numbers of metastatic sites. The presence of miRNA-126 is important for maintaining blood vessel integrity [19, 30], and an association with MVD has been reported in CRC as well [31]. The blood vessel integrity should, consequently, be lower in tumours with low miRNA-126 expression levels which, in turn, may facilitate the entering of cancer cells into the blood circulation. A recent report on this topic fully supports this hypothesis [32].

Current knowledge on miRNA-126 suggests that it is essential for several angiogenic processes. The ability of a tumour to regulate miRNA-126 expression may be important during multiple phases of the metastatic process, such as the entering of tumour cells into the lymph- and/or bloodstream, the extravasation into distant organs and the subsequent induction of angiogenesis in order for the colonization of the metastatic cells to be successful. The delivery of chemotherapy to the malignant tumour entails another scenario, in which the blood vessel structure is known to be of importance [33, 34]. The increased interstitial tumour pressure that follows low blood vessel integrity will hamper the passage of macromolecules such as cytostatics from the blood vessel compartment to the tumour cells, which provides an explanation of the lower response rate observed among these patients.

With these notions in mind, there might be a causal relationship between miRNA-126 expression at the invasive tumour front, the number of metastatic sites and, subsequently, the response to chemotherapy. A less pronounced relationship was also observed in our previous study in which we assessed miRNA-126 expression in the entire tumour area [23]. Further detailed analyses of the relationships between miRNA-126 expression, tumour response, and metastases will require larger cohort studies.

The present analyses are based on histological examinations of the primary tumours, and do not involve metastatic lesions. Interestingly, all these primary tumours were removed by surgery before chemo-therapeutic intervention, indicating a relationship between the miRNA-126 MVDi estimate and the efficacy of the treatment targeting the remaining tumour burden (i.e., the metastasis). This suggests that cellular and/or molecular characteristics of the primary tumour may be retained at the metastatic sites [35, 36]. The correlation observed between miRNA-126 MVDi and treatment response translated into a significant difference in PFS when patients were divided into groups according to the median miRNA-126 MVDi. A marginally significant relationship with OS was also detected. A multivariate analysis was not appropriate based on the limited size of the current study cohort and the lack of obvious prognostic markers in the clinical setting of advanced, metastatic disease. Hence, the possible prognostic value of the miRNA-126 MVDi needs further exploration in appropriately sized cohorts.

MicroRNA-126 and CD34 constitute the biological basis of the EC parameters tested, and represent two different ways of estimating the angiogenic activity. The expression of miRNA-126 is especially pronounced in ECs [21], whereas CD34 is a cell adhesion molecule expressed in different cells besides ECs (i.e., tissue stem cells, myoepithelial cells, mesenchymal cells, inflammatory cells etc.) [37, 38]. Although most CD34 positive cells in the CRC tissue sections seem to be ECs, we also noted a certain contribution from stromal fibroblastic cells. Hence, the visualisation of these two markers may lead to the quantification of two compartments not entirely identical and this, in turn, may explain the lack of correlation between the estimates and their differences in predicting therapy response. Adding to this, differences in quantification techniques and sizes of the areas estimated may have resulted in four very different estimates. While both markers, miRNA-126 and CD34, provide numerical estimates of the angiogenetic activity in the respective tumours, miRNA-126 may also add information about blood vessel integrity [19, 30].

Although miRNA-126 MVDi provided the most promising results in the current study, more studies are needed to substantiate miR-126 MVDi as a valid therapy response biomarker. Several methodological aspects of the quantitative miRNA ISH assay require elucidation and should be taken into account when interpreting the results. Factors that could influence the final results include surgical handling of the specimen, time of ischemia, fixation and storage of the tissue, experimental parameters in the ISH analysis, and normalization of the semi-quantitative results obtained by the image guided analyses. The relatively high stability of microRNA in FFPE material [39] may facilitate retrospective studies to substantiate the strength of the miR-126 MVDi parameter.

Although the retrospective design and the size of the current study pose limitations, our results underline the technological difficulties in obtaining clinically useful MVD estimates in tissue sections from CRC patients. Different technical approaches have a profound impact on the ultimate data obtained. We showed that both the methodological assessment of MVD and the molecular endothelial marker used are imperative for predicting chemotherapy response in mCRC. The miRNA-126 MVDi estimate was the only biomarker related to response in patients with mCRC treated with first-line XELOX, suggesting that MVDi represents a clinical biomarker superior to MVDh. Future studies on samples obtained from treatment regimens based on chemotherapy plus bevacizumab will be needed to address the question whether the miRNA-126 MVDi estimate can be used for treatment stratification within this context.

Acknowledgments We are very thankful for the technical assistance provided by Birgit Roed Sørensen and Stine Jørgensen, and for the linguistic editing provided by Karin Larsen. Furthermore, René dePont Christensen is acknowledged for statistical counselling. This study was supported by The Cancer Foundation and The Danish Council for Independent Research, which did not affect any part of the study.

Conflict of interest The authors declare that they have no conflict of interests.

References

1. D. Hanahan, R.A. Weinberg, The hallmarks of cancer. Cell **100**, 57–70 (2000)
2. R.T. Tong, Y. Boucher, S.V. Kozin, F. Winkler, D.J. Hicklin, R.K. Jain, Vascular normalization by vascular endothelial growth factor receptor 2 blockade induces a pressure gradient across the vasculature and improves drug penetration in tumors. Cancer Res. **64**, 3731–3736 (2004)
3. H. Wildiers, G. Guetens, B.G. De, E. Verbeken, B. Landuyt, B. Landuyt, E.A. Bruijn, A.T. van Oosterom, Effect of antivascular endothelial growth factor treatment on the intratumoral uptake of CPT-11. Br. J. Cancer **88**, 1979–1986 (2003)
4. C.G. Willett, D.G. Duda, E. di Tomaso, Y. Boucher, B.G. Czito, Z. Vujaskovic, G. Vlahovic, J. Bendell, K.S. Cohen, H.I. Hurwitz, Complete pathological response to bevacizumab and chemoradiation in advanced rectal cancer. Nat. Clin. Pract. Oncol. **4**, 316–321 (2007)
5. K. Akagi, Y. Ikeda, Y. Sumiyoshi, Y. Kimura, J. Kinoshita, M. Miyazaki, T. Abe, Estimation of angiogenesis with anti-CD105

immunostaining in the process of colorectal cancer development. Surgery **131**, S109–S113 (2002)
6. G.G. Des, B. Uzzan, P. Nicolas, M. Cucherat, J.F. Morere, R. Benamouzig, J.L. Breau, G.Y. Perret, Microvessel density and VEGF expression are prognostic factors in colorectal cancer. Meta-analysis of the literature. Br. J. Cancer **94**, 1823–1832 (2006)
7. P. Bossi, G. Viale, A.K. Lee, R. Alfano, G. Coggi, S. Bosari, Angiogenesis in colorectal tumors: microvessel quantitation in adenomas and carcinomas with clinicopathological correlations. Cancer Res. **55**, 5049–5053 (1995)
8. Y. Takebayashi, S. Aklyama, K. Yamada, S. Akiba, T. Aikou, Angiogenesis as an unfavorable prognostic factor in human colorectal carcinoma. Cancer **78**, 226–231 (1996)
9. L. Hlatky, P. Hahnfeldt, J. Folkman, Clinical application of antiangiogenic therapy: microvessel density, what it does and doesn't tell us. J. Natl. Cancer Inst. **94**, 883–893 (2002)
10. E. Fonsatti, V.L. Del, M. Altomonte, L. Sigalotti, M.R. Nicotra, S. Coral, P.G. Natali, M. Maio, Endoglin: an accessory component of the TGF-beta-binding receptor-complex with diagnostic, prognostic, and bioimmunotherapeutic potential in human malignancies. J. Cell. Physiol. **188**, 1–7 (2001)
11. D.W. Miller, W. Graulich, B. Karges, S. Stahl, M. Ernst, A. Ramaswamy, H.H. Sedlacek, R. Muller, J. Adamkiewicz, Elevated expression of endoglin, a component of the TGF-beta-receptor complex, correlates with proliferation of tumor endothelial cells. Int. J. Cancer **81**, 568–572 (1999)
12. R. Minhajat, D. Mori, F. Yamasaki, Y. Sugita, T. Satoh, O. Tokunaga, Endoglin (CD105) expression in angiogenesis of colon cancer: analysis using tissue microarrays and comparison with other endothelial markers. Virchows Arch. **448**, 127–134 (2006)
13. D. Royston, D.G. Jackson, Mechanisms of lymphatic metastasis in human colorectal adenocarcinoma. J. Pathol. **217**, 608–619 (2009)
14. A. Esquela-Kerscher, F.J. Slack, Oncomirs - microRNAs with a role in cancer. Nat. Rev. Cancer **6**, 259–269 (2006)
15. W. Filipowicz, S.N. Bhattacharyya, N. Sonenberg, Mechanisms of post-transcriptional regulation by microRNAs: are the answers in sight? Nat. Rev. Genet. **9**, 102–114 (2008)
16. J.E. Fish, D. Srivastava, MicroRNAs: opening a new vein in angiogenesis research. Sci. Signal. **2**, pe1 (2009)
17. A. Kuehbacher, C. Urbich, A.M. Zeiher, S. Dimmeler, Role of Dicer and Drosha for endothelial microRNA expression and angiogenesis. Circ. Res. **101**, 59–68 (2007)
18. S. Jorgensen, A. Baker, S. Moller, B.S. Nielsen, Robust one-day in situ hybridization protocol for detection of microRNAs in paraffin samples using LNA probes. Methods **52**, 375–381 (2010)
19. J.E. Fish, M.M. Santoro, S.U. Morton, S. Yu, R.F. Yeh, J.D. Wythe, K.N. Ivey, B.G. Bruneau, D.Y. Stainier, D. Srivastava, miR-126 regulates angiogenic signaling and vascular integrity. Dev. Cell **15**(272–284) (2008)
20. S. Wang, A.B. Aurora, B.A. Johnson, X. Qi, J. McAnally, J.A. Hill, J.A. Richardson, R. Bassel-Duby, E.N. Olson, The endothelial-specific microRNA miR-126 governs vascular integrity and angiogenesis. Dev. Cell **15**, 261–271 (2008)
21. E. Wienholds, W.P. Kloosterman, E. Miska, E. Alvarez-Saavedra, E. Berezikov, E. de Bruijn, H.R. Horvitz, S. Kauppinen, R.H. Plasterk, MicroRNA expression in zebrafish embryonic development. Science **309**, 310–311 (2005)
22. B.S. Nielsen, S. Jorgensen, J.U. Fog, R. Sokilde, I.J. Christensen, U. Hansen, N. Brunner, A. Baker, S. Moller, H.J. Nielsen, High levels of microRNA-21 in the stroma of colorectal cancers predict short disease-free survival in stage II colon cancer patients. Clin. Exp. Metastasis **28**, 27–38 (2011)
23. T.F. Hansen, F.B. Soerensen, J. Lindebjerg, A. Jakobsen, The predictive value of microRNA-126 in relation to first line treatment with capecitabine and oxaliplatin in patients with metastatic colorectal cancer. BMC Cancer **12**, 83 (2012)
24. S. Hansen, D.A. Grabau, C. Rose, M. Bak, F.B. Sorensen, Angiogenesis in breast cancer: a comparative study of the observer variability of methods for determining microvessel density. Lab. Invest. **78**, 1563–1573 (1998)
25. R. Rajaganeshan, R. Prasad, P.J. Guillou, C.R. Chalmers, N. Scott, R. Sarkar, G. Poston, D.G. Jayne, The influence of invasive growth pattern and microvessel density on prognosis in colorectal cancer and colorectal liver metastases. Br. J. Cancer **96**, 1112–1117 (2007)
26. A.A. Romani, A.F. Borghetti, R.P. Del, M. Sianesi, P. Soliani, The risk of developing metastatic disease in colorectal cancer is related to CD105-positive vessel count. J. Surg. Oncol. **93**, 446–455 (2006)
27. T.F. Hansen, F.B. Sorensen, K.L. Spindler, D.A. Olsen, R.F. Andersen, J. Lindebjerg, I Brandslund, A Jakobsen, Microvessel density and the association with single nucleotide polymorphisms of the vascular endothelial growth factor receptor 2 in patients with colorectal cancer. Virchows Arch. **456**, 251–260 (2010)
28. H. Hurwitz, L. Fehrenbacher, W. Novotny, T. Cartwright, J. Hainsworth, W. Heim, J. Berlin, A. Baron, S. Griffing, E. Holmgren, Bevacizumab plus irinotecan, fluorouracil, and leucovorin for metastatic colorectal cancer. N. Engl. J. Med. **350**, 2335–2342 (2004)
29. C.J. Allegra, G. Yothers, M.J. O'Connell, S. Sharif, N.J. Petrelli, L.H. Colangelo, J.N. Atkins, T.E. Seay, L. Fehrenbacher, R.M. Goldberg, Phase III trial assessing bevacizumab in stages II and III carcinoma of the colon: results of NSABP protocol C-08. J. Clin. Oncol. **29**, 11–16 (2011)
30. S. Nicoli, C. Standley, P. Walker, A. Hurlstone, K.E. Fogarty, N.D. Lawson, MicroRNA-mediated integration of haemodynamics and Vegf signalling during angiogenesis. Nature **464**, 1196–2000 (2010)
31. T.F. Hansen, C.L. Andersen, B.S. Nielsen, K.L. Spindler, F.B. Sorensen, J. Lindebjerg, I. Brandslund, A. Jakobsen, Elevated microRNA-126 is associated with high vascular endothelial growth factor receptor 2 expression levels and high microvessel density in colorectal cancer. Oncol Lett **2**, 1101–1106 (2011)
32. K.J. Png, N. Halberg, M. Yoshida, S.F. Tavazoie, A microRNA regulon that mediates endothelial recruitment and metastasis by cancer cells. Nature **481**, 190–194 (2011)
33. R.K. Jain, Normalization of tumor vasculature: an emerging concept in antiangiogenic therapy. Science **307**, 58–62 (2005)
34. R.K. Jain, Normalizing tumor vasculature with anti-angiogenic therapy: a new paradigm for combination therapy. Nat. Med. **7**, 987–989 (2001)
35. V. Kulda, M. Pesta, O. Topolcan, V. Liska, V. Treska, A. Sutnar, K. Rupert, M. Ludvikova, V. Babuska, L. Holubec Jr., Relevance of miR-21 and miR-143 expression in tissue samples of colorectal carcinoma and its liver metastases. Cancer Genet. Cytogenet. **200**, 154–160 (2010)
36. M.M. Vickers, J. Bar, I. Gorn-Hondermann, N. Yarom, M. Daneshmand, J.E. Hanson, C.L. Addison, T.R. Asmis, D.J. Jonker, J. Maroun, Stage-dependent differential expression of microRNAs in colorectal cancer: potential role as markers of metastatic disease. Clin. Exp. Metastasis **29**, 123–132 (2011)
37. A.E. Lindenmayer, M. Miettinen, Immunophenotypic features of uterine stromal cells. CD34 expression in endocervical stroma. Virchows Arch. **426**, 457–460 (1995)
38. M. Van de Rijn, R.V. Rouse, CD34. Appl Immunohistochem **2**, 71–80 (1994)
39. Y. Xi, G. Nakajima, E. Gavin, C.G. Morris, K. Kudo, K. Hayashi, J. Ju, Systematic analysis of microRNA axpression of RNA extracted from fresh frozen and formalin-fixed paraffin-embedded samples. RNA **13**, 1668–1674 (2007)